



ELSEVIER

Journal of Non-Crystalline Solids 262 (2000) 276–281

 JOURNAL OF
 NON-CRYSTALLINE SOLIDS

www.elsevier.com/locate/jnoncrysol

Letter to the Editor

Dynamic thermal expansivity near the glass transition

C. Bauer ^{a,1}, R. Richert ^{a,2}, R. Böhmer ^{a,*}, T. Christensen ^b^a *Institut für Physikalische Chemie, Johannes Gutenberg-Universität, 55099 Mainz, Germany*^b *IMFUFU, Roskilde University Centre, Postbox 260, 4000 Roskilde, Denmark*

Received 6 July 1999; received in revised form 15 October 1999

Abstract

Dielectric techniques were used to investigate the thermal expansivity of polystyrene films. Capacitive scanning dilatometry (CSD) employs temperature ramping in order to monitor the non-linear structural relaxation in the glass transformation range and to quantify liquid fragility. In the linear response regime, the complex thermal expansivity is obtained as a function of the temperature cycling frequency and is observed to reflect the structural relaxation. © 2000 Elsevier Science B.V. All rights reserved.

PACS: 65.70 + y; 77.22.Ch; 64.70.Pf

Thermodynamic properties of supercooled liquids and polymers undergo significant changes in the glass transformation range. Therefore, heat capacity, compressibility, and thermal expansivity are often used to monitor the vitrification process. Consequently, there exist a number of experimental techniques to determine these quantities in the quasi-static limit [1]. It has long been recognized that their frequency or time dependences should also be mapped out in order to gain deeper insights into the kinetic nature of the glass transition [2]. In this respect, the determination of the dynamic heat capacity under either temperature scanning [3] or temperature cycling conditions has

received particular attention (see the collection of articles published in [4]). Also the methods to record the adiabatic compressibility in a broad frequency range were recently refined considerably [5]. On the other hand, we do not know of an experimental report ³ on the explicit frequency dependence of the thermal expansivity, $\alpha(\omega)$. ⁴ Therefore, we have developed a simple technique to measure $\alpha(\omega)$ employing harmonic temperature modulation. The changes in sample geometry are monitored in terms of the capacitance of the electrode/sample assembly and also allow to perform experiments under temperature ramping conditions. This latter technique, which we call capacitive scanning dilatometry (CSD), yields

* Corresponding author. Tel.: +49-6131 392 2536; fax: +49-6131 392 4196.

E-mail address: bohmer@aak.chemie.uni-mainz.de (R. Böhmer).

¹ Present address: Fachbereich Physik, Philipps-Universität, 35032 Marburg, Germany.

² Present address: Department of Chemistry and Biochemistry, Arizona State University, Tempe, AZ 85287-1604, USA.

³ The frequency-dependent thermal expansivity of a supercooled Lennard–Jones liquid was recently studied by Nielsen [6].

⁴ The temporal evolution of volume (or related quantities) of glass-forming materials induced by temperature steps was measured early on, e.g., by Jenckel [7].

information analogous to differential scanning calorimetry (DSC) [3,4].

For our novel technique the sample itself, in this case a polymer film, serves to define the separation of the electrode pair. Such an arrangement is much simpler than most approaches described before (very recently CSD was used to study very thin polymer films [8,9]). The price one has to pay for this simplicity is that the measuring signal, i.e., the capacitance of the electroded film, under adverse conditions does not only reflect dilatometric but also dielectric properties. However, as we will show below, one can disentangle these effects by a suitable choice of experimental parameters. The possibility of simultaneously accessing the dilatometric and dielectric properties in a single experiment avoids ambiguities encountered when comparing data from different sources. In particular, such a combined measurement allows for a simple quantification of fragility, a key parameter for characterizing glass-forming liquids [10]. As was shown very recently, a similar approach can be devised using DSC techniques, but then requires auxiliary equipment [11].

For our initial experiments we have chosen polystyrene (PS), a standard polymer, but polybutadiene (PB) and polyvinylacetate (PVAc) have been studied as well [12]. Thin films (1–10 μm thick) were produced by spin coating or drop casting atactic PS ($M_w = 119,000$ g/mol) using glass or metal substrates. The active electrode area of the capacitors ranged from 30 to 80 mm^2 . No significant differences between differently prepared films were found. The capacitor assemblies, with calibrated Pt-sensors attached in close proximity to the polymer films, were thermostatted using a commercial system from Novocontrol. Using the standard regulation capabilities of our system we achieved cooling or heating rates of $0.1 \text{ K/min} < |q| < 4.5 \text{ K/min}$. Smaller rates were reached by repeatedly stepping the temperature typically by 0.15 K and subsequent stabilization. The maximum cycling frequency was 10 mHz. The experiments were carried out using temperature oscillation amplitudes of 0.2–0.7 K. In Ref. [12] we find an approximate linearity of response up to oscillation amplitudes of about 1.4 K, in agreement with results from thermomodulated DSC

experiments [13,14]. For the measurement of the dielectric constant we employed a Solartron SI-1260 gain/phase analyzer equipped with a Mestec DM-1360 transimpedance amplifier. It is stressed, however, that any other system capable of monitoring capacitance for frequencies larger than about 100 kHz at a comparable resolution would be suitable for the present purpose. Unless stated otherwise, we utilized a detection frequency f_D near 450 kHz.

For a first characterization of the PS films, we monitored the capacitance upon cooling at a rate of $q = -0.08 \text{ K/min}$. The results obtained for several frequencies, f_D , are shown in the inset of Fig. 1. For the highest f_D we find a change of slope near the calorimetric glass transition temperature. For lower f_D this effect is superimposed by dielectric dispersion showing up in the real part of the

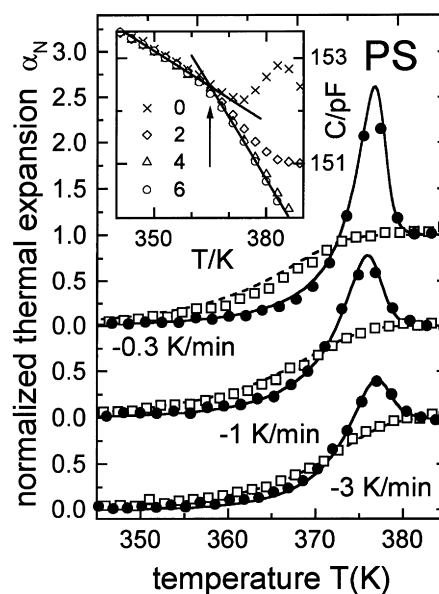


Fig. 1. Symbols represent the normalized thermal expansion, $\alpha_N(T)$, obtained by cooling down to 328 K at various rates (see labels) and immediate reheating with 3 K/min. The lines are from calculations within the Narayanaswamy–Moynihan approach described in the text and provide a good description of our measurements. The inset depicts the frequency dependent capacitance as recorded upon cooling with $q = -0.08 \text{ K/min}$. The numbers in the inset give the frequencies as $\log_{10}(f/\text{Hz})$. The straight lines are drawn to represent the linear dependences of C in the glassy and in the liquid regimes. The arrow marks their intersection from which T_g can be read off.

dielectric constant. From this data the frequency range suitable for the present purpose can readily be recognized. In order to extract the coefficient of linear thermal expansion, α , from the temperature-dependent high-frequency capacitance, $C(T)$, two considerations need to be made. The derivative, $dC/dT = \epsilon_\infty dC_0/dT + C_0 d\epsilon_\infty/dT$, contains one contribution from the change in the geometric capacitance, C_0 , and another one from the density dependence of the dielectric constant itself. Since we are dealing with the dielectric constant, ϵ_∞ , at frequencies above the regime of orientational polarization, we may apply the Lorenz–Lorentz equation in order to evaluate the latter effect. Using this approach one can derive [12] $\alpha = N^{-1}(dC/dT)_A$ with $N = C_0[\epsilon_\infty + (\epsilon_\infty - 1)(\epsilon_\infty + 2)/3]$. The subscript A is meant as a reminder that the constant ‘area’, i.e., the thin film expansivity rather than the constant pressure coefficient, α_p , is of interest here. The two are related via $\alpha = \alpha_p(1 + \nu)/(1 - \nu)$ [15]. The difference in the explicit frequency or temperature dependences of α and α_p is relatively small because the temperature variation of the term involving the Poisson ratio, ν , is about a factor of 10 smaller than that of α . Using published values (we utilized $\nu = 0.33$ for the glassy state and $\nu = 0.5$ for the liquid, see [16]) for ν and the observed slopes, dC/dT , marked by the straight lines in Fig. 1, we find that in the glassy state $\alpha_{p,g} = (7.0 \pm 0.5) \times 10^{-5} \text{ K}^{-1}$ and that in the liquid $\alpha_{p,l} = (15.5 \pm 1.0) \times 10^{-5} \text{ K}^{-1}$ in good agreement with the literature.⁵ Using the two limiting values one can compute the normalized coefficient, $\alpha_N(T) = [\alpha(T) - \alpha_g]/\Delta\alpha$, with $\Delta\alpha = \alpha_l - \alpha_g$.

In Fig. 1 we show $\alpha_N(T)$ as measured for various cooling rates and subsequent reheating with 3 K/min. A pronounced hysteresis between downscan and upscan as well as the development of an overshoot are noted. The latter feature becomes most prominent for slow precooling. Similar effects are well known from DSC investi-

gations which are usually analyzed within the fictive temperature approach. In an analogous fashion we write $\alpha_N = dT_f/dT$ and derive the fictive temperature, T_f , within the Adam–Gibbs approach modified according to Scherer [17]. As the solid lines in Fig. 1 show, α_N obtained for several thermal histories can be described excellently using the parameters derived from previous DSC experiments on PS (we used $\ln(\tau_0/s) = -63.5$, $B = 7630 \text{ K}$, $T_2 = 260 \text{ K}$, and $\beta = 0.54$ as given by Hodge [18]).

The frequency-dependent thermal expansivity was determined from the capacitance modulation amplitude, ΔC , generated by a harmonic temperature excursion of magnitude ΔT . From the amplitude ratio and the phase lag between $C(t)$ and $T(t)$ of our polymer samples we computed the real and imaginary parts of $\alpha(\omega) = \alpha'(\omega) + i\alpha''(\omega)$ for several temperature cycling frequencies, ω , employing digital lock-in techniques. By using various modulation amplitudes we ascertained that our experiment operates in the linear response

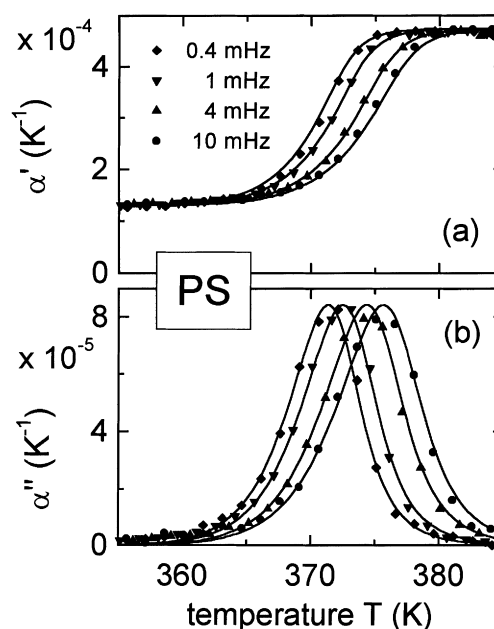


Fig. 2. (a) In-phase and (b) out-of-phase components of the complex thin film thermal expansion coefficient. The temperature modulation frequencies are indicated. Lines are fits based on Havriliak–Negami and Vogel–Fulcher expressions with the parameters given in the text.

⁵ Our $\alpha_{p,l}$ is about 10% smaller than the published one, probably indicating that the assumption of a constant area is a good approximation, only. Then, in the liquid state the polymer film will not perfectly stick to the substrate, hence be able to slightly expand into the lateral directions, and lead to a minor decrease of the longitudinal expansion.

regime. In Fig. 2 we show the results obtained for $0.4 \text{ mHz} \leq \omega/2\pi \leq 10 \text{ mHz}$. In the real part of the expansivity, α' , we observe well-defined steps, while in α'' frequency-dependent peaks show up. Via the relation $\omega\tau \approx 1$ the peak maxima indicate the time scale, τ , on which the expansivity response takes place at a certain temperature. In Fig. 3 we plot the modulation frequencies versus peak temperatures. The solid line through the data represents a shift factor of 2.9 K/decade [19]. Additionally, Fig. 3 reveals that the rate-dependent glass transition temperatures (determined from the break in slope of the $C(T)$ curve; cf. inset of Fig. 1) for a given cooling rate are compatible with the same shift factor. The ordinate axes of Fig. 3 are plotted in a way which allows to compare frequencies ω (or relaxation times τ) with the associated cooling rates. One can see that, e.g., $q = -10 \text{ K/min}$ (left-hand scale of Fig. 3) and $\omega/2\pi = 0.4 \text{ mHz}$ (right-hand scale) correspond to the same temperature. This is a direct experimental

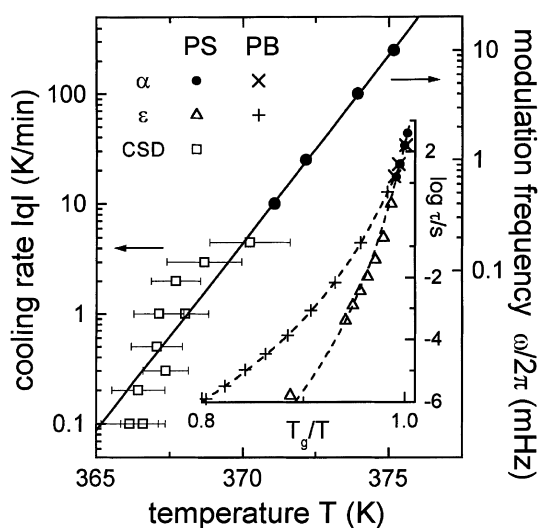


Fig. 3. Characteristic freezing (or glass transition) temperatures of PS as obtained under various experimental conditions. The scale on the left-hand side refers to T_g determinations from capacitive scanning dilatometry (cf. inset of Fig. 1). Data from the modulation experiments (full circles) obtained from the maxima of α'' (cf. Fig. 2) correspond to the axis on the right-hand side. The straight line represents a shift factor of 2.9 K/decade. The inset is an Angell plot for PB [12] and PS incorporating relaxation times obtained from the maxima in α'' and in ε'' . The dashed lines are fits using Vogel–Fulcher expressions.

indication that a rate of 10 K/min corresponds to an average structural relaxation time τ ($= \omega^{-1}$) of about 400 s.⁶ The order of magnitude of this correspondence is in agreement with simple theoretical estimates [3,21,22].

In the inset of Fig. 3 the time scales from our dilatometric results are compared with the inverse peak frequencies from dielectric spectroscopy recorded for the same specimen. Both sets of data can be described using the same Vogel–Fulcher (VF) equation, $\tau = \tau_0 \exp[DT_2/(T - T_2)]$, with $\log_{10}(\tau_0/s) = -13.8$, $DT_2 = 685 \text{ K}$, and $T_2 = 329 \text{ K}$.⁷ From these quantities the fragility index m can be computed [24]. Alternatively, the fragility parameter [25] $F_{1/2} = 2T_g/T_{1/2} - 1$ can be read off directly from the experimental data. Here T_g and $T_{1/2}$ denote the temperatures corresponding to time scales of 10^2 and 10^{-6} s , respectively. For PS we find $F_{1/2} = 0.79$. Fig. 3 also includes results from our recent study on PB [12], for which $F_{1/2} = 0.60$ is obtained. A straightforward alternative route for assessing $F_{1/2}$ is to measure the capacitance $C(T)$ at a fixed frequency $2\pi f_D = 10^6 \text{ Hz}$ over a temperature range which includes T_g and $T_{1/2}$. As we have demonstrated for PB [12], the resulting $C(T)$ displays a kink at T_g due to the dilatometric effects and a step at $T_{1/2}$ associated with orientational dielectric polarization. Thereby, $F_{1/2}$ is readily obtained from fixed frequency impedance measurements performed over a limited temperature interval.

Since the characteristic time scales for the dilatometric and dielectric responses agree rather well, the question arises whether the spectral widths are also comparable. In order to resolve this issue in Fig. 4 we show Cole–Cole plots of the normalized complex expansivity as well as of the complex dielectric constant of PS. In both cases skewed arcs are seen which can be parameterized using the Havriliak–Negami (HN) formula, $\alpha_N(\omega) = \alpha'_N(\omega) + i\alpha''_N(\omega) = [1 + (i\omega\tau)^\delta]^{-\gamma}$, or the corresponding expression for the analogously

⁶ A similar estimate for PS was performed by Hensel and Schick [20], who determine T_g from the midpoint of DSC curves. These authors find that a rate of 10 K/min corresponds to a time scale of 125 s.

⁷ Parameters from cycling and ramping experiments can be different as discussed for glycerol by Moynihan et al. [23].

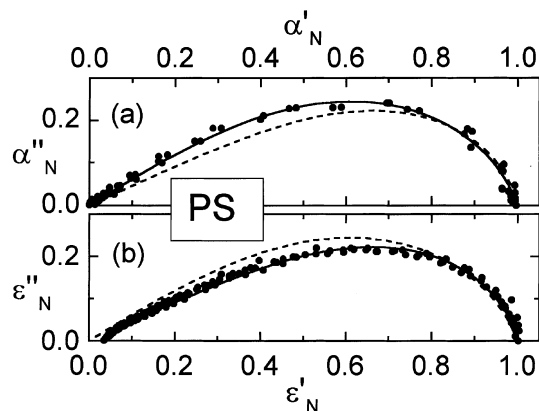


Fig. 4. Cole–Cole plot of the normalized (a) dilatometric and (b) dielectric susceptibilities. The lines are calculated with the Havriliak–Negami expression and the parameters given in the text. In each frame the upper line corresponds to $\alpha_N(\omega)$ and the lower one to $\epsilon_N(\omega)$.

normalized dielectric constant, $\epsilon_N(\omega)$. The result of this procedure is shown by the lines in Fig. 4. We find $\delta = 0.78$, $\gamma = 0.45$ for $\alpha_N(\omega)$ and $\delta' = 0.85$, $\gamma' = 0.32$ for $\epsilon_N(\omega)$. The $\alpha''_N(\omega)$ vs. $\alpha'_N(\omega)$ plot rests on the $\alpha(T, \omega)$ data of Fig. 2, but allows for determining the HN parameters without explicitly referring to $\tau(T)$. Combining these shape parameters with a VF fit for $\tau(T)$ leads to the solid lines in Fig. 2. In the relevant temperature range, the VF fits for the dielectric (τ_ϵ) and expansivity (τ_α) time scales agree within 0.1 decades.

The above numbers for the HN exponents δ and γ translate into (FWHM) widths of $w_\alpha = 2.3$ for $\alpha_N(\omega)$ and $w_\epsilon = 2.5$ for $\epsilon_N(\omega)$ as regards the imaginary parts on a $\log_{10}(\omega)$ scale. A heat capacity spectroscopy study of PS ($M_w = 270,000$ g/mol) reported by Korus et al. [26,27] leads to $w_c = 2.1$ for the effusivity $\rho c_p(\omega)$. There is no firm theoretical basis for expecting identical τ and w values obtained from different experimental approaches. The present results $\tau_\alpha \approx \tau_\epsilon$ and $w_\alpha \approx w_\epsilon$ suggest that the dynamic expansivity, like various other relaxation types, is intimately coupled to the primary or structural relaxation.

In summary, we have demonstrated the possibilities of monitoring subtle changes in the geometry of thin polymer films using capacitance measurements. The combination of this technique with temperature ramping or harmonic tempera-

ture oscillations allows to evaluate the capacitance changes in terms of the dynamic expansivity, $\alpha(\omega)$. Already a simplified model leads to quantitative agreement of $\alpha_{p,g}$ and $\alpha_{p,l}$ with literature values. Both the average time scale, τ , and the loss profile, $\alpha''(\omega)$, are found compatible with the structural relaxation of PS. Because both characteristic temperatures, T_g and $T_{1/2}$, show up in a temperature sweep of $C(2\pi f_D = 10^6$ Hz), this technique is particularly straightforward for assessing the fragility, $F_{1/2}$, of polymer films. A future higher resolution version of this experimental approach might reveal the dynamical expansivity associated with β -relaxations in glassy materials.

Acknowledgements

We thank T. Christensen, G. Diezemann, S. Moreno-Flores, D. Neher, N.B. Olsen, and H. Sillescu for stimulating discussions and J.K. Nielsen for communicating Ref. [6] prior to publication.

References

- [1] J.D. Ferry, *Viscoelastic Properties of Polymers*, Wiley, New York, 1980.
- [2] C.T. Moynihan et al., *Ann. New York Acad. Sci.* 279 (1976) 15.
- [3] I.M. Hodge, *J. Non-Cryst. Solids* 169 (1994) 211.
- [4] *Thermochim. Acta* 304&305 (1997).
- [5] T. Christensen, N.B. Olsen, *Phys. Rev. B* 49 (1994) 15396.
- [6] J.K. Nielsen, *Phys. Rev. E* 60 (1999) 471.
- [7] E. Jenckel, *Z. Elektrochem.* 43 (1937) 796.
- [8] K. Fukao, Y. Miyamoto, *Europhys. Lett.* 46 (1999) 649.
- [9] K. Fukao, Y. Miyamoto, *Phys. Rev. E*, in press.
- [10] K. Ito, C.T. Moynihan, C.A. Angell, *Nature* 398 (1999) 492.
- [11] K. Ito, J.L. Green, K. Xu, C.A. Angell, *J. Phys. Chem. B* 103 (1999) 3991.
- [12] C. Bauer, R. Böhmer, S. Moreno-Flores, R. Richert, H. Sillescu, D. Neher, *Phys. Rev. E*, in press.
- [13] J.E.K. Schawe, S. Theobald, *J. Non-Cryst. Solids* 235–237 (1998) 496.
- [14] C. Schick, M. Merzlyakov, A. Hensel, *J. Chem. Phys.* 111 (1999) 2695.
- [15] W.E. Wallace, J.H. van Zanten, W.L. Wu, *Phys. Rev. B* 52 (1995) R3329.
- [16] J. Brandrup, E.H. Immergut (Eds.), *Polymer Handbook*, 2nd Ed., Wiley, New York, 1975.

- [17] G.W. Scherer, *J. Am. Ceram. Soc.* 67 (1984) 504.
- [18] I.M. Hodge, *Macromolecules* 20 (1987) 2897.
- [19] R. Greiner, F.R. Schwarzl, *Rheolog. Acta* 23 (1984) 378.
- [20] A. Hensel, C. Schick, *J. Non-Cryst. Solids* 235–237 (1998) 510.
- [21] A. Pimenov, R. Böhmer, A. Loidl, *Prog. Theor. Phys. Suppl.* 126 (1997) 185.
- [22] J.M. Hutchinson, S. Montserrat, *Thermochim. Acta* 304&305 (1997) 257.
- [23] C.T. Moynihan, S.N. Crichton, J.M. Opalka, *J. Non-Cryst. Solids* 131–133 (1991) 420.
- [24] R. Böhmer, C.A. Angell, *Phys. Rev. B* 48 (1993) 5857.
- [25] R. Richert, C.A. Angell, *J. Chem. Phys.* 108 (1998) 9016.
- [26] J. Korus, thesis, Universität Halle, 1997.
- [27] S. Weyer, A. Hensel, J. Korus, E. Donth, C. Schick, *Thermochim. Acta* 304&305 (1997) 251.